



Brain iron deposition in type 2 diabetes mellitus with and without mild cognitive impairment—an in vivo susceptibility mapping study

Qifang Yang^{1,2} · Lina Zhou³ · Chen Liu¹ · Daihong Liu¹ · Yang Zhang¹ · Chang Li¹ · Yongning Shang¹ · Xin Wei¹ · Chuanming Li¹ · Jian Wang¹

Published online: 3 January 2018
© Springer Science+Business Media, LLC, part of Springer Nature 2018

Abstract

This study was performed to investigate iron deposition in the brain of type 2 diabetes mellitus (T2DM) patients using quantitative susceptibility mapping (QSM) and the associated cognitive impairments. Sixty patients diagnosed with T2DM were subjected to neuropsychological tests to determine their cognitive status, and the results were used to subdivide the patients into a T2DM without mild cognitive impairment (MCI) group (n = 30) and a T2DM with MCI group (n = 30). All patients underwent high-resolution susceptibility-weighted imaging, and data processing was performed using SMART (Susceptibility Mapping and Phase Artifacts Removal Toolbox) software. The susceptibility values of the bilateral parietal cortex, frontal white matter, caudate nucleus (CN), putamen (PU), globus pallidus, thalamus, red nucleus, substantia nigra (SN), hippocampus (HP) and dentate nucleus were analyzed and correlated with the neuropsychological cognitive scores. Compared with the normal controls (n = 30), the T2DM without MCI group exhibited significantly increased susceptibility values in the left HP, whereas the T2DM with MCI group showed significantly increased susceptibility values in the bilateral CN, HP, left PU and right SN. Compared with the T2DM without MCI group, the T2DM with MCI group exhibited significantly increased susceptibility values in the right CN, SN and left PU. The susceptibility values for the right CN, SN and left PU were closely correlated with neuropsychological cognitive scores. Our results provide a new relation between T2DM and brain iron deposition and suggested that QSM may be a helpful tool in the detection and evaluation of their cognitive impairment in T2DM.

Keywords Type 2 diabetes mellitus · Magnetic resonance imaging · Susceptibility mapping · Cognitive impairment · Iron deposition

Introduction

Type 2 diabetes mellitus (T2DM) is a long-term metabolic disorder characterized by high blood sugar, insulin resistance, and a relative lack of insulin. In 2015, more than 400 million people were living with diabetes worldwide, and the number is increasing in every country (Whiting et al. 2011). In addition to the well-known connection between T2DM and peripheral nervous system disease, diabetes may also induce central nervous system lesions. Patients with T2DM can have cognitive deficits in many domains, such as executive functions, memory, attention, and visuospatial abilities (Kodl and Seaquist 2008). T2DM is an independent risk factor for Alzheimer's disease (AD), vascular dementia (VaD) and mild cognitive impairment (MCI) (Smith et al. 2010; Moon et al. 2016). However, the mechanism

Qifang Yang and Lina Zhou contributed equally to this work.

✉ Chuanming Li
li_chuanming@yeah.net

✉ Jian Wang
wangjian_811@yahoo.com

¹ Department of Radiology, Southwest Hospital, Third Military Medical University, Chongqing, China

² Department of Medical imaging, PLA No.44 Hospital, Guizhou, China

³ Department of Endocrinology, Southwest Hospital, Third Military Medical University, Chongqing, China

underlying the influence of T2DM on the functions of specific brain regions has not been fully elucidated.

Iron contributes to many biological processes, including oxygen transport, protein expression regulation, and cell growth. In the brain, iron plays a central role in brain development, neurotransmitter systems, and myelin synthesis. Recently, a number of studies have demonstrated that excessive iron deposition in the brain plays an important role in the emergence and development of cognitive impairment (Smith et al. 1997; Duce et al. 2010; Haller et al. 2010). Iron deposition is frequently observed in T2DM, in close association with the development of T2DM and its complications (Wang et al. 2014). Prospective clinical studies have demonstrated that body iron storage is positively correlated with the prevalence of T2DM (Forouhi et al. 2007; Montonen et al. 2012). Nevertheless, iron deposition has not been studied in the brains of T2DM patients.

Iron is a paramagnetic element that can strengthen the local externally applied magnetic field. Several magnetic resonance imaging (MRI) methods have been developed to measure iron deposition in the brain, such as T2*-weighted (T2*W) imaging and phase imaging. Recently, Haacke et al. (Haacke et al. 2010, 2015) presented quantitative susceptibility mapping (QSM) technology that reliably quantifies tissue iron concentrations, and the results are consistent with histopathologic examinations (Bilgic et al. 2012; Yan et al. 2013; Chai et al. 2015; Xia et al. 2015). This study was performed to investigate iron deposition in the brain of T2DM with and without MCI, using QSM of MR.

Materials and methods

Subjects

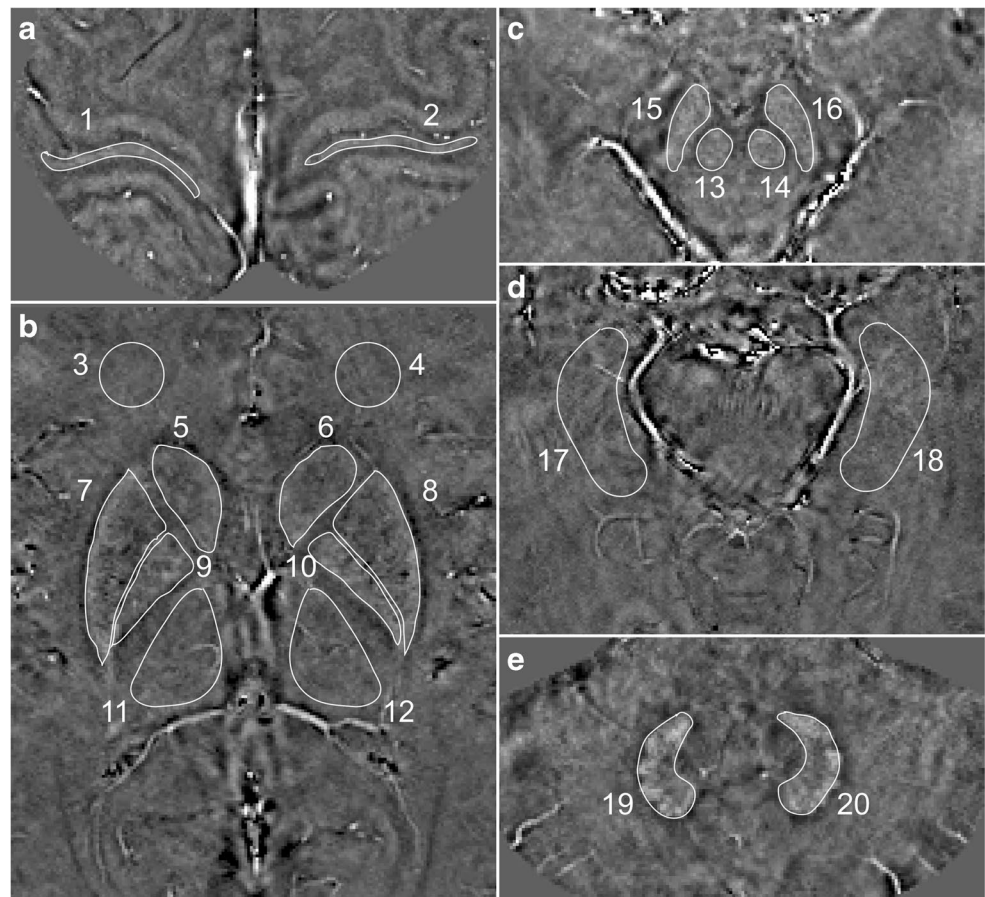
Sixty patients diagnosed with T2DM were recruited from our hospital between March 2015 and June 2016. T2DM was diagnosed according to the criteria proposed by the World Health Organization 1999 (Group 1999). The 60 patients were subdivided into the T2DM without MCI group ($n = 30$) and the T2DM with MCI group ($n = 30$). The MCI was defined according to the criteria proposed by Petersen, including complaints of hypomnesia, Mini Mental State Examination (MMSE) score > 24 , Montreal Cognitive Assessment (MoCA) score < 26 , clinical dementia rating (CDR) ≥ 0.5 and normal activities of daily living (ADL) score (Petersen 2004; Zhou et al. 2015; Zheng et al. 2016; Li et al. 2016). Thirty normal controls with no history of nervous system disease, vascular risk factors, cognitive complaints, or psychiatric illness were recruited through advertisements and were matched with above groups in terms of age, sex and education. All of the participants were right-handed. And the exclusion criteria included (1) alcoholism,

brain injury, Parkinson's disease, epilepsy, major depression, or other neurological or psychiatric disorders; (2) microvascular complications, including retinopathy, nephropathy or neuropathy; and (3) severe depression (Hamilton Depression Rating Scale ≥ 18), dementia (MMSE < 24), severe claustrophobia, or contraindications to MRI. To estimate the sub-domains of cognition, all participants underwent neuropsychological examinations as follows: Auditory Verbal Learning Test (AVLT), Complex Figure Test (CFT), Digit Symbol Coding Test (DSCT), Digit Span Test (DST), Verbal Fluency Test (VFT), and Trail-Making Test parts A and B (TMT-A and TMT-B). Clinical data were also recorded in all participants, including the height, weight, body mass index (BMI) and blood pressure. Furthermore, the fasting glucose, glycosylated hemoglobin (HbA1c), total cholesterol, triglycerides, high density lipoprotein (HDL) cholesterol and low density lipoprotein (LDL) cholesterol were known as risk factors for cognitive dysfunction (McCrimmon et al. 2012). So these clinical parameters were measured by standard laboratory testing. Written informed consent to participate in this study was obtained from all participants. The study was approved by the Medical Ethics Committee of our hospital and conducted in accordance with the Declaration of Helsinki.

Magnetic resonance imaging

All of the subjects were subjected to MRI on a 3.0 T whole body system (Magnetom Trio, Siemens Healthcare, Erlangen, Germany) equipped with a twelve-channel phase-array head coil. Susceptibility-weighted images (SWI) were obtained using a high-resolution three-dimensional spoiled gradient-echo sequence with the following parameters: TR/TE, 29/20 ms; flip angle, 15° ; section thickness, 2 mm; field of view, 256×256 cm; and matrix size, 512×512 . SMART (Susceptibility Mapping and Phase Artifacts Removal Toolbox, Detroit, MI, USA) and SPIN (signal processing in nuclear magnetic resonance, MR Innovations Inc., Detroit, MI, USA) software were used for the data processing and measurement (Haacke et al. 2004; Pandian et al. 2008). First, the phase images were processed with a 32×32 high pass filter and zero filled. Then, skull stripping and complex thresholding were used to remove noise outside the brain. Finally, a 0.1 threshold regularized inverse filter was applied to prevent ill-defined regions of k-space. Regions of interest (ROI) were manually drawn on every slice of the bilateral parietal cortex (PC), frontal white matter (FWM), caudate nucleus (CN), putamen (PU), globus pallidus (GP), thalamus (TH), red nucleus (RN), substantia nigra (SN), hippocampus (HP), and dentate nucleus (DN) (Fig. 1). The ROI in the FWM was circular and had an area of 100 pixels. T1-weighted images were obtained with the following parameters: TR/TE, 200/2.78 ms; flip angle, 70° ; matrix,

Fig. 1 Regions of interest (ROI) depicted on the quantitative susceptibility mapping (QSM) images. 1, 2 = parietal cortex (PC); 3, 4 = frontal white matter (FWM); 5, 6 = caudate nucleus (CN); 7, 8 = putamen (PU); 9, 10 = globus pallidus (GP); 11, 12 = thalamus (TH); 13, 14 = red nucleus (RN); 15, 16 = substantia nigra (SN); 17, 18 = hippocampus (HP); and 19, 20 = dentate nucleus (DN)



384 × 384; thickness, 5.0 mm; and voxel size, 0.9 × 0.7 × 5 mm³. The FLAIR sequence was scanned using the following parameters: TR/TE/TI, 9000/93/2500 ms; flip angle, 130°; matrix, 256 × 256; thickness, 4.0 mm; and voxel size: 0.9 × 0.9 × 4 mm³. White matter lesion severity was assessed on FLAIR images using the age-related white matter changes scale (Wahlund et al. 2001) by agreement of two experienced neurologists. Participants with a rating score of above one (confluence of lesions or diffuse involvement of the entire region) were excluded (Cui et al. 2015).

Statistical analysis

Statistical analyses were performed using SPSS software (version 18.0; SPSS, Inc., Chicago, IL, USA). The distribution of the data was analyzed using the Kolmogorov–Smirnov test. Comparisons of the demographic data, clinical data, cognitive scores and susceptibility values among the three groups were performed using analyses of variance (ANOVAs) for normally distributed continuous data, and the *LSD* test was used for the post hoc analysis. The *Kruskal–Wallis H* test was used for non-normally distributed or unequal variances data, and the *Mann–Whitney U* test was used for the post hoc analysis, with the significance level (α)

adjusted by the Bonferroni correction. A χ^2 test was used to compare proportions, and an independent two-sample *t*-test was used to assess the diabetes duration. Partial correlations between the susceptibility values and neuropsychological test scores, including scores for the MMSE, MoCA, AVLT, CFT, DSCT, DST, VFT, and TMT tests, were analyzed for the T2DM with MCI group. The age, gender and education level of each subject were imported as covariates in the statistical analysis. The *p* values were considered significant at <0.05.

Results

The three groups did not differ significantly in age, gender, education, BMI, systolic blood pressure, diastolic blood pressure, total cholesterol, LDL cholesterol, white matter lesions, AVLT-delayed recall (5 min), AVLT-delayed recall (20 min), DST-forwards, VFT or MMSE scores ($p > 0.05$). Compared with the normal controls, the T2DM without MCI group had higher fasting glucose, HbA1c and lower HDL cholesterol and MoCA scores. While compared with the T2DM without MCI group, the T2DM with MCI group had higher scores of TMT-A, TMT-B tests and lower scores

of AVLT, CFT-delayed recall (20 min), DSCT, and MoCA tests (Table 1).

The susceptibility values in the FWM, CN, PU, GP, TH, RN, SN and HP subregions of our 30 normal controls were -1.051 , 7.914 , 7.143 , 22.053 , 4.777 , 30.15 , 16.490 , and -1.429 ppb ($\times 10^{-9}$), respectively, and the postmortem brain iron concentrations in the corresponding subregions reported by Hallgren and Sourander were 4.24 , 9.28 , 13.32 , 21.30 , 4.76 , 19.48 , 18.64 , and 3.13 mg per 100 grams of wet weight, respectively (Hallgren and Sourander 1958). Thus, a close positive correlation was observed between our susceptibility values and the actual iron concentrations in brain regions reported in the literature ($r = 0.915$, $p = 0.001$; Fig. 2a). This result demonstrated our brain iron

deposition data was reliable and accurate. The ANOVA results indicated that the susceptibility values in the bilateral CN, HP, left PU and right SN were significantly different among the three groups ($p < 0.05$). Compared with the normal controls, the T2DM without MCI group exhibited significantly increased susceptibility values in the left HP. The T2DM with MCI group showed significantly increased susceptibility values in the bilateral CN, HP, left PU and right SN. While compared with the T2DM without MCI group, the T2DM with MCI group exhibited significantly increased susceptibility values in right CN, SN and left PU (Table 2). The right CN susceptibility values were closely correlated with the AVLT-delayed recall (5 min) scores ($r = -0.450$, $p = 0.019$; Fig. 2b), the AVLT-delayed recall

Table 1 Demographic, clinical data and cognitive scores of all subjects

	NC (n=30)	T2DM without MCI (n=30)	T2DM with MCI (n=30)	p value
Age (years)	53.17 ± 6.57	54.97 ± 5.54	55.9 ± 6.54	0.231
Sex (male/female) ¹	14/16	19/11	12/18	0.177
Education (years)	11.80 ± 2.99	11.90 ± 2.92	10.43 ± 2.94	0.105
Diabetes duration (years) ²	—	7.93 ± 5.98	6.93 ± 5.46	0.502
BMI (kg/m ²)	24.12 ± 2.49	24.34 ± 2.83	25.04 ± 3.27	0.437
Systolic blood pressure (mmHg)	128.13 ± 18.10	131.37 ± 14.78	130.57 ± 18.25	0.749
Diastolic blood pressure (mmHg)	79.77 ± 9.17	82.90 ± 9.80	80.60 ± 10.33	0.441
Fasting glucose (mmol/L) ³	5.47 ± 0.63	8.56 ± 1.97	9.14 ± 3.05	0.000* ^{ab}
HbA _{1c} (%) ³	5.50 ± 0.36	8.84 ± 1.72	9.13 ± 2.07	0.000* ^{ab}
Total cholesterol (mmol/L)	5.21 ± 0.96	4.96 ± 1.37	5.24 ± 1.45	0.651
Triglyceride (mmol/L) ³	1.12(0.96–2.01)	1.49(1.02–2.73)	2.03(1.37–3.27)	0.021* ^b
HDL cholesterol (mmol/L)	1.40 ± 0.33	1.18 ± 0.30	1.16 ± 0.33	0.008* ^{ab}
LDL cholesterol (mmol/L)	3.10 ± 0.67	2.93 ± 0.78	3.36 ± 1.06	0.160
White matter lesions ³	0 (0–5)	1(0–6)	1(0–7)	0.584
AVLT	22.83 ± 5.00	22.77 ± 3.83	19.50 ± 4.55	0.006* ^{bc}
AVLT-delayed recall (5 min) ³	8.20 ± 1.94	7.80 ± 1.56	7.23 ± 2.40	0.249
AVLT-delayed recall (20 min)	7.87 ± 2.18	7.33 ± 1.77	6.83 ± 2.64	0.204
CFT-immediate recall	24.08 ± 8.49	22.63 ± 6.95	19.00 ± 6.64	0.027* ^b
CFT-delayed recall (20 min)	23.65 ± 7.74	21.85 ± 7.13	18.20 ± 6.19	0.012* ^{bc}
DSCT	46.23 ± 11.99	41.23 ± 10.83	35.63 ± 8.33	0.001* ^{bc}
DST-forwards ³	9.57 ± 1.38	8.87 ± 0.82	8.93 ± 1.08	0.117
DST-backwards	5.53 ± 1.17	5.03 ± 0.91	4.67 ± 0.88	0.004* ^b
VFT	44.83 ± 6.06	44.10 ± 8.29	40.60 ± 7.05	0.057
TMT-A	48.57 ± 16.61	51.97 ± 17.44	63.80 ± 21.66	0.006* ^{bc}
TMT-B	61.33 ± 22.74	67.73 ± 24.19	80.77 ± 26.60	0.010* ^{bc}
MoCA ³	27.77 ± 1.28	27.00 ± 0.83	22.93 ± 1.95	0.000* ^{abc}
MMSE	28.43 ± 1.17	28.43 ± 1.07	27.93 ± 1.31	0.176

Data are presented as the means ± SD for normally distributed data and the median(range) for non-normally distributed data. *Abbreviations:* AVLT Auditory Verbal Learning Test, CFT Complex Figure Test, DSCT Digit Symbol Coding Test, DST Digit Span Test, VFT Verbal Fluency Test, TMT Trail Making Test, MMSE Mini-Mental State Examination, and MoCA Montreal Cognitive Assessment. ¹The p value was obtained using the χ^2 test. ²The p value was obtained using the independent two-sample t -test. ³The p value was obtained using the Kruskal-Wallis H test, and the Mann-Whitney U test was used for the post hoc analysis, with the significance level (α) adjusted by the Bonferroni correction. * $p < 0.05$. ^aSignificant differences between the NC and T2DM without MCI groups. ^bSignificant differences between the NC and T2DM with MCI groups. ^cSignificant differences between the T2DM without MCI and T2DM with MCI groups.

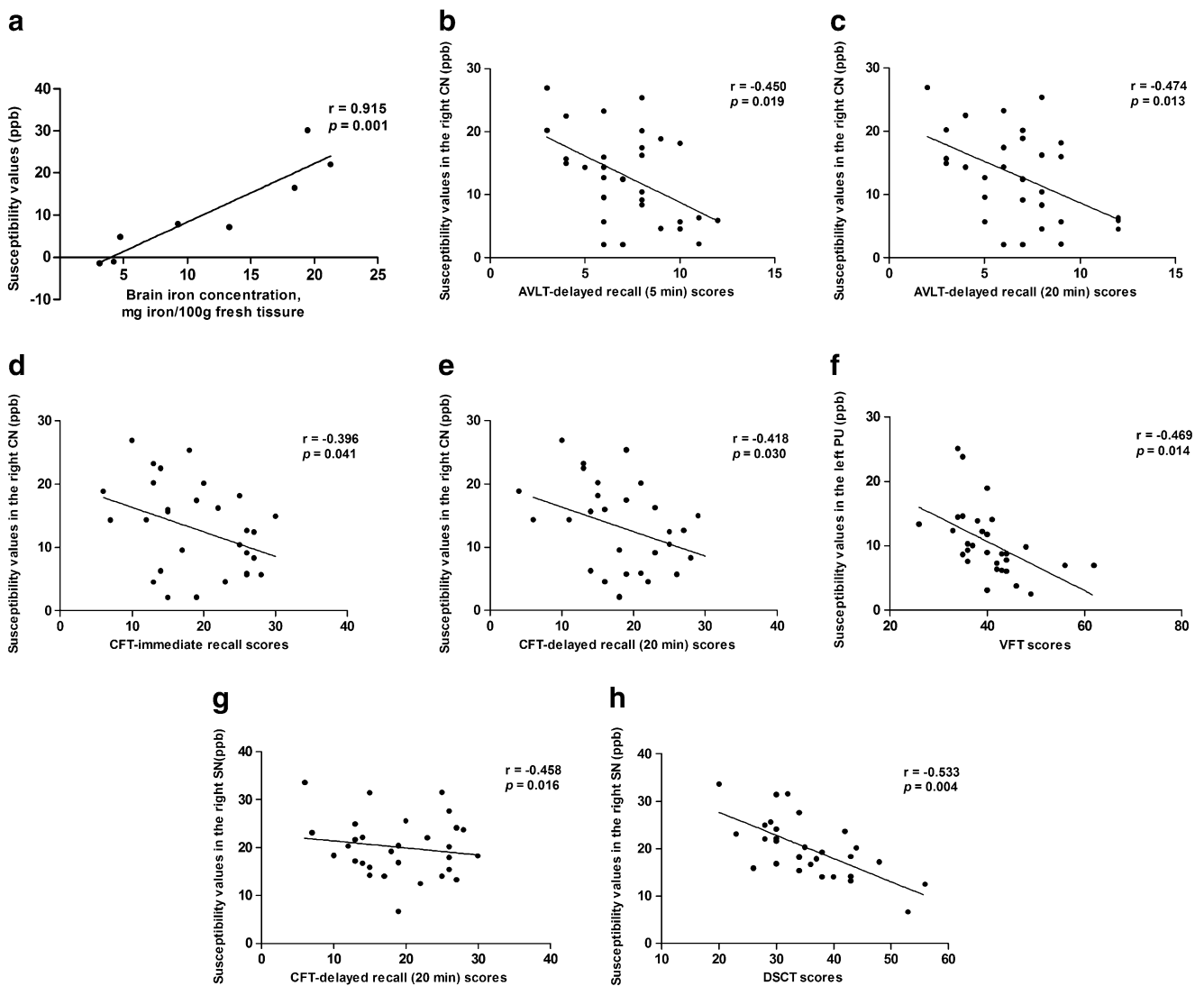


Fig. 2 **a**: Correlation between the brain susceptibility values of the 30 normal controls and the real postmortem brain iron concentrations reported by Hallgren and Sourander ($r=0.915$, $p=0.001$). **b–e**: Correlations between the susceptibility values in the right CN and the AVLT-delayed recall (5 min) scores, the AVLT-delayed recall (20 min) scores, the CFT-immediate recall scores and the CFT-

delayed recall (20 min) scores of the T2DM with MCI patients. **f**: Correlations between the susceptibility values in the left PU and the VFT scores of the T2DM with MCI patients. **g–h**: Correlations between the susceptibility values in the right SN and the CFT-delayed recall (20 min) scores, the DSCT scores of the T2DM with MCI patients

(20 min) scores ($r = -0.474$, $p = 0.013$; Fig. 2c), the CFT-immediate recall (20 min) scores ($r = -0.396$, $p = 0.041$; Fig. 2d), and the CFT-delayed recall (20 min) scores ($r = -0.418$, $p = 0.030$; Fig. 2e); the left PU susceptibility values were closely correlated with the VFT scores ($r = -0.469$, $p = 0.014$; Fig. 2f); and the right SN susceptibility values were closely correlated with the CFT-delayed recall (20 min) scores ($r = -0.458$, $p = 0.0016$; Fig. 2g) and the DSCT scores ($r = -0.533$, $p = 0.004$; Fig. 2h).

Discussion

Iron deposition can lead to altered magnetic field heterogeneities relative to the surrounding parenchyma, which can be detected by SWI and QSM in vivo (Langkammer et al. 2012). SWI is more accurate than T2-weighted, T2*-weighted, and R2* mapping for iron quantification and has been used to evaluate brain iron deposition associated with normal aging and several brain diseases

Table 2 Susceptibility values [ppb ($\times 10^{-9}$)] differences among the three groups

ROI	NC (n=30)	T2DM without MCI(n=30)	T2DM with MCI(n=30)	p value	p value for post hoc analysis		
					a	b	c
Right PC	19.12 ± 6.13	20.32 ± 5.17	19.23 ± 5.90	0.672	0.420	0.937	0.467
Left PC	20.40 ± 5.90	21.69 ± 6.25	20.60 ± 5.90	0.673	0.410	0.900	0.484
Right FWM	-1.18 ± 2.88	0.07 ± 2.80	0.05 ± 3.40	0.193	0.114	0.120	0.979
Left FWM	-0.92 ± 2.53	-0.27 ± 2.65	0.35 ± 3.21	0.223	0.372	0.084	0.397
Right CN	7.65 ± 5.30	8.50 ± 5.61	12.84 ± 7.23	0.003*	0.593	0.001*	0.007*
Left CN	8.17 ± 4.99	9.51 ± 6.28	12.54 ± 6.88	0.021*	0.398	0.007*	0.058
Right PU	6.82 ± 3.98	7.58 ± 5.19	7.68 ± 6.39	0.790	0.581	0.530	0.939
Left PU	7.47 ± 4.09	7.65 ± 4.70	10.44 ± 5.31	0.028*	0.884	0.017*	0.025*
Right GP	21.56 ± 6.22	20.86 ± 6.67	19.27 ± 6.15	0.361	0.666	0.164	0.335
Left GP	22.54 ± 7.51	22.56 ± 8.22	21.42 ± 7.92	0.816	0.991	0.585	0.578
Right TH	4.75 ± 3.96	4.67 ± 4.78	4.87 ± 5.28	0.986	0.945	0.922	0.867
Left TH	4.80 ± 3.83	4.98 ± 4.83	4.62 ± 4.90	0.953	0.878	0.876	0.757
Right RN	31.04 ± 12.45	28.88 ± 11.19	33.68 ± 13.21	0.322	0.497	0.409	0.134
Left RN	29.26 ± 11.60	29.55 ± 13.29	32.39 ± 12.13	0.557	0.927	0.328	0.375
Right SN	15.65 ± 7.49	15.87 ± 8.00	20.09 ± 6.09	0.032*	0.907	0.020*	0.027*
Left SN	17.33 ± 9.51	19.06 ± 9.47	20.85 ± 6.84	0.297	0.441	0.120	0.429
Right HP	-1.10 ± 3.25	0.13 ± 2.99	0.97 ± 2.62	0.028*	0.112	0.008*	0.273
Left HP	-1.76 ± 2.99	-0.12 ± 2.86	0.74 ± 3.41	0.008*	0.044*	0.002*	0.283
Right DN	16.73 ± 6.54	15.69 ± 5.76	19.09 ± 9.15	0.186	0.584	0.212	0.074
Left DN	17.64 ± 8.98	16.18 ± 6.26	20.16 ± 8.75	0.162	0.485	0.231	0.060

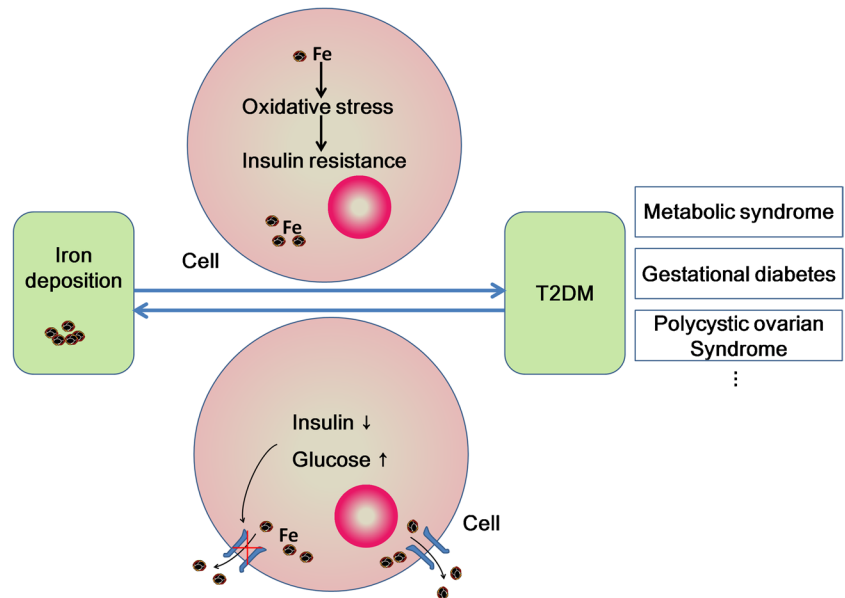
Data are presented as the means ± SD. Susceptibility values for the three groups were compared using an ANOVA analysis. a=NC - T2DM without MCI, b=NC - T2DM with MCI, c=T2DM without MCI-T2DM with MCI. *p<0.05. PC, parietal cortex; FWM, frontal white matter; CN, caudate nucleus; PU, putamen; GP, globus pallidus; TH, thalamus; RN, red nucleus; SN, substantia nigra; HP, hippocampus; DN, dentate nucleus

(Achiriloaie et al. 2011; Bilgic et al. 2012; Langkammer et al. 2012; Schweser et al. 2012). Previously, Hallgren and Sourander (Hallgren and Sourander 1958) performed autopsy examinations on 81 normal brains and quantitatively measured the iron concentrations of different brain regions using chemical colorimetry, and their data have been proposed as the gold standard for brain iron concentration investigations. In this study, we found a close correlation between the regional susceptibility values in the CN, PU, GP, TH, SN, RN and FWM of our normal controls and the real brain iron concentrations published by Hallgren and Sourander. This result demonstrated our brain iron deposition data was reliable and accurate.

To our knowledge, this is the first study to investigate T2DM-related brain iron deposition. Because brain iron levels can increase with age in healthy individuals, we used age-matched controls to eliminate this effect. Given that there was no white matter changes scale difference among three groups, the iron deposition may reflect the cognitive impairment purely. Compared with the T2DM patients without cognitive impairment, the T2DM patients with MCI showed more iron deposition in the right CN, SN and left PU, and the susceptibility of these structures

was closely correlated with cognitive impairment. Our results provide a new relation between T2DM and brain iron deposition, which suggested that iron deposition may play an important role in the process of T2DM cognitive impairment and QSM may be a helpful tool in the detection and evaluation of it. The PU is part of the basal ganglia and connected to the cerebral cortex and brainstem. This structure controls voluntary movement and is involved in several cognitive functions, such as memory, emotion, and learning. Lesions in the PU can lead to a variety of cognitive impairments (Bastos-Leite et al. 2007; Kantarci et al. 2010). The SN plays an important role in reward, movement, learning and addiction, and it is involved in the dorsolateral prefrontal circuit, which is responsible for executive functions. Iron deposition in these regions can catalyze free radicals and promote lipid peroxidation, which can induce oxidative stress injury and neural lesions. Excessive iron accumulation has been proved to induce neuronal function lesions and connectivity disruption (Rouault 2001; Salazar et al. 2008; Schweser et al. 2012). MCI was reported to be associated with iron accumulation in different brain regions, and different stages of MCI show different iron depositions (Haller et al.

Fig. 3 Iron deposition may result in insulin resistance via oxidative stress which can produce damage to cells. And the insulin resistance is related to T2DM, metabolic syndrome, gestational diabetes, and polycystic ovarian syndrome. Meanwhile, the elevated glucose level may obstruct the outflow of iron in cells, which may aggravate the iron deposition



2010). At the molecular level iron also play a significant role in neurodegenerative disease. A recent meta-analysis found that an elevated ratio of copper to non-heme iron in subjects with MCI predicted who would progress to Alzheimer's disease (Schrage et al. 2013). Plascencia-Villa's study demonstrate that Fe in Formation of amyloid- β plaque cores is present iron oxide (Fe_3O_4) magnetite nanoparticles (Plascencia-Villa et al. 2016).

In this study, compared with the normal controls, the T2DM without MCI patients showed significantly higher iron deposition in the left HP. Our results are generally consistent with the previous literatures. The HP has been shown to be specifically affected both structurally and functionally in T2DM patients (Gold et al. 2007; Bruehl et al. 2009). Compared with the normal controls, significant atrophy was observed in the HP of the T2DM patients (Zhang et al. 2015). Increases in creatinine and myo-inositol in the HP have also been observed in Zucker Diabetic Fatty rats (van der Graaf et al. 2004). The precise mechanisms underlying the higher iron concentration in T2DM are not understood. High body iron levels have been found associated with increased levels of oxidative stress, which may elevate the risk of T2DM. Epidemiological studies have shown a positive association between high body iron stores and the risk of insulin-resistant states, such as T2DM, metabolic syndrome, gestational diabetes, and polycystic ovarian syndrome (Sam et al. 2013; Sampaio et al. 2014; Zein et al. 2014). On the other hand, the relationship between iron metabolism and T2DM appears to be bidirectional (Fig. 3). Iron can affect glucose metabolism via its deleterious effect on pancreatic cells, and glucose metabolism can impair several iron metabolic pathways (Biessels et al. 1998; Fernandez-Real et al. 2002).

In conclusion, in this study we found iron depositions in several brain regions including the bilateral CN, HP, left PU and right SN in patients with T2DM. The susceptibility values of the right CN, SN and left PU were closely correlated with their cognitive impairment. Our results provide a new relation between T2DM and brain iron deposition, which suggested that iron deposition may play an important role in the process of T2DM cognitive impairment and QSM may be a helpful tool in the detection and evaluation of it. The main limitation is the relatively small sample size. Secondly, because of the cross-sectional design, we were unable to observe the dynamics of iron deposition. Longitudinal studies of T2DM patients with larger samples of different stages of cognitive impairment should be conducted in the future.

Funding This work was supported by the National Natural Science Foundation of China (No. 81471647 and No. 81771814) and the Forefront & Applied Basic Research Foundation of Chongqing City (No. cstc2014jcyjA0884).

Compliance with ethical standards

Conflict of interest The authors declare no conflict of interest.

Ethical approval All procedures performed in this study were in accordance with the ethical standards of our institutional research committee and with the 1964 Helsinki declaration and its later amendments. Informed consent was obtained from all individual participants included in the study.

References

Achiriloaie, A. F., Kido, D., Wycliffe, D., & Jacobson, J. P. (2011). White matter microsusceptibility changes in patients with

- hepatic encephalopathy. *Journal of Radiology Case Reports*, 5(8), 1–7. <https://doi.org/10.3941/jrcr.v5i8.393>.
- Bastos-Leite, A. J., van der Flier, W. M., van Straaten, E. C., Staekenborg, S. S., Scheltens, P., & Barkhof, F. (2007). The contribution of medial temporal lobe atrophy and vascular pathology to cognitive impairment in vascular dementia. *Stroke*, 38(12), 3182–3185. <https://doi.org/10.1161/STROKEAHA.107.490102>.
- Biessels, G. J., Kamal, A., Urban, I. J., Spruijt, B. M., Erkelens, D. W., & Gispen, W. H. (1998). Water maze learning and hippocampal synaptic plasticity in streptozotocin-diabetic rats: effects of insulin treatment. *Brain Research*, 800(1), 125–135. [https://doi.org/10.1016/S0006-8993\(98\)00510-1](https://doi.org/10.1016/S0006-8993(98)00510-1).
- Bilgic, B., Pfefferbaum, A., Rohlfing, T., Sullivan, E. V., & Adalsteinsson, E. (2012). MRI estimates of brain iron concentration in normal aging using quantitative susceptibility mapping. *Neuroimage*, 59(3), 2625–2635. <https://doi.org/10.1016/j.neuroimage.2011.08.077>.
- Bruehl, H., Wolf, O. T., Sweat, V., Tirsi, A., Richardson, S., & Convit, A. (2009). Modifiers of cognitive function and brain structure in middle-aged and elderly individuals with type 2 diabetes mellitus. *Brain Research*, 1280, 186–194. <https://doi.org/10.1016/j.brainres.2009.05.032>.
- Chai, C., Zhang, M., Long, M., Chu, Z., Wang, T., Wang, L., et al. (2015). Increased brain iron deposition is a risk factor for brain atrophy in patients with haemodialysis: a combined study of quantitative susceptibility mapping and whole brain volume analysis. *Metabolic Brain Disease*, 30(4), 1009–1016. <https://doi.org/10.1007/s11011-015-9664-2>.
- Cui, Y., Jiao, Y., Chen, H. J., Ding, J., Luo, B., Peng, C. Y., et al. (2015). Aberrant functional connectivity of default-mode network in type 2 diabetes patients. *European Radiology*. <https://doi.org/10.1007/s00330-015-3746-8>.
- Duce, J. A., Tsatsanis, A., Cater, M. A., James, S. A., Robb, E., Wikke, K., et al. (2010). Iron-export ferroxidase activity of beta-amyloid precursor protein is inhibited by zinc in Alzheimer's disease. *Cell*, 142(6), 857–867. <https://doi.org/10.1016/j.cell.2010.08.014>.
- Fernandez-Real, J. M., Lopez-Bermejo, A., & Ricart, W. (2002). Cross-talk between iron metabolism and diabetes. *Diabetes*, 51(8), 2348–2354.
- Forouhi, N. G., Harding, A. H., Allison, M., Sandhu, M. S., Welch, A., Luben, R., et al. (2007). Elevated serum ferritin levels predict new-onset type 2 diabetes: results from the EPIC-Norfolk prospective study. *Diabetologia*, 50(5), 949–956. <https://doi.org/10.1007/s00125-007-0604-5>.
- Gold, S. M., Dziobek, I., Sweat, V., Tirsi, A., Rogers, K., Bruehl, H., et al. (2007). Hippocampal damage and memory impairments as possible early brain complications of type 2 diabetes. *Diabetologia*, 50(4), 711–719. <https://doi.org/10.1007/s00125-007-0602-7>.
- Group, W. C. (1999). *Definition, diagnosis and classification of diabetes mellitus and its complications*. Geneva: World Health Organization.
- Haacke, E. M., Liu, S., Buch, S., Zheng, W., Wu, D., & Ye, Y. (2015). Quantitative susceptibility mapping: current status and future directions. *Magnetic Resonance Imaging*, 33(1), 1–25. <https://doi.org/10.1016/j.mri.2014.09.004>.
- Haacke, E. M., Tang, J., Neelavalli, J., & Cheng, Y. C. (2010). Susceptibility mapping as a means to visualize veins and quantify oxygen saturation. *Journal of Magnetic Resonance Imaging*, 32(3), 663–676. <https://doi.org/10.1002/jmri.22276>.
- Haacke, E. M., Xu, Y., Cheng, Y. C., & Reichenbach, J. R. (2004). Susceptibility weighted imaging (SWI). *Magnetic Resonance in Medicine*, 52(3), 612–618. <https://doi.org/10.1002/mrm.20198>.
- Haller, S., Bartsch, A., Nguyen, D., Rodriguez, C., Emch, J., Gold, G., et al. (2010). Cerebral microhemorrhage and iron deposition in mild cognitive impairment: susceptibility-weighted MR imaging assessment. *Radiology*, 257(3), 764–773. <https://doi.org/10.1148/radiol.10100612>.
- Hallgren, B., & Sourander, P. (1958). The effect of age on the non-haemin iron in the human brain. *Journal of Neurochemistry*, 3(1), 41–51.
- Kantarci, K., Avula, R., Senjem, M. L., Samikoglu, A. R., Zhang, B., Weigand, S. D., et al. (2010). Dementia with Lewy bodies and Alzheimer disease: neurodegenerative patterns characterized by DTI. *Neurology*, 74(22), 1814–1821. <https://doi.org/10.1212/WNL.0b013e3181e0f7cf>.
- Kodl, C. T., & Seaquist, E. R. (2008). Cognitive dysfunction and diabetes mellitus. *Endocrine Reviews*, 29(4), 494–511. <https://doi.org/10.1210/er.2007-0034>.
- Langkammer, C., Schweser, F., Krebs, N., Deistung, A., Goessler, W., Scheurer, E., et al. (2012). Quantitative susceptibility mapping (QSM) as a means to measure brain iron? a post mortem validation study. *Neuroimage*, 62(3), 1593–1599. <https://doi.org/10.1016/j.neuroimage.2012.05.049>.
- Li, W., Wang, T., & Xiao, S. (2016). Type 2 diabetes mellitus might be a risk factor for mild cognitive impairment progressing to Alzheimer's disease. *Neuropsychiatric Disease and Treatment*, 12, 2489–2495. <https://doi.org/10.2147/ndt.s111298>.
- Liu, C., Li, C., Yang, J., Gui, L., Zhao, L., Evans, A. C., et al. (2015). Characterizing brain iron deposition in subcortical ischemic vascular dementia using susceptibility-weighted imaging: an in vivo MR study. *Behavioural Brain Research*, 288, 33–38. <https://doi.org/10.1016/j.bbr.2015.04.003>.
- McCrimmon, R. J., Ryan, C. M., & Frier, B. M. (2012). Diabetes and cognitive dysfunction. [Review]. *Lancet*, 379(9833), 2291–2299. [https://doi.org/10.1016/S0140-6736\(12\)60360-2](https://doi.org/10.1016/S0140-6736(12)60360-2).
- Montonen, J., Boeing, H., Steffen, A., Lehmann, R., Fritsche, A., Joost, H. G., et al. (2012). Body iron stores and risk of type 2 diabetes: results from the European Prospective Investigation into cancer and nutrition (EPIC)-potdam study. *Diabetologia*, 55(10), 2613–2621. <https://doi.org/10.1007/s00125-012-2633-y>.
- Moon, Y., Han, S. H., & Moon, W. J. (2016). Patterns of brain iron accumulation in vascular dementia and alzheimer's dementia using quantitative susceptibility mapping imaging. *Journal of Alzheimer's Disease*, 51(3), 737–745. <https://doi.org/10.3233/JAD-151037>.
- Nakada, T., Matsuzawa, H., Igarashi, H., Fujii, Y., & Kwee, I. L. (2008). In vivo visualization of senile-plaque-like pathology in Alzheimer's disease patients by MR microscopy on a 7T system. *Journal of Neuroimaging*, 18(2), 125–129. <https://doi.org/10.1111/j.1552-6569.2007.00179.x>.
- Pandian, D. S., Ciulla, C., Haacke, E. M., Jiang, J., & Ayaz, M. (2008). Complex threshold method for identifying pixels that contain predominantly noise in magnetic resonance images. *Journal of Magnetic Resonance Imaging*, 28(3), 727–735. <https://doi.org/10.1002/jmri.21487>.
- Petersen, R. C. (2004). Mild cognitive impairment as a diagnostic entity. *Journal of Internal Medicine*, 256(3), 183–194. <https://doi.org/10.1111/j.1365-2796.2004.01388.x>.
- Plascencia-Villa, G., Ponce, A., Collingwood, J. F., Arellano-Jimenez, M. J., Zhu, X., Rogers, J. T., et al. (2016). High-resolution analytical imaging and electron holography of magnetite particles in amyloid cores of Alzheimer's disease. *Scientific Reports*, 6, 24873. <https://doi.org/10.1038/srep24873>.
- Rouault, T. A. (2001). Iron on the brain. *Nature Genetics*, 28(4), 299–300. <https://doi.org/10.1038/91036>.
- Salazar, J., Mena, N., Hunot, S., Prigent, A., Alvarez-Fischer, D., Arredondo, M., et al. (2008). Divalent metal transporter 1 (DMT1) contributes to neurodegeneration in animal models of Parkinson's disease. *Proceedings of the National Academy of Sciences of the United States of America*, 105(47), 18578–18583. <https://doi.org/10.1073/pnas.0804373105>.

- Sam, A. H., Busbridge, M., Amin, A., Webber, L., White, D., Franks, S., et al. (2013). Hepcidin levels in diabetes mellitus and polycystic ovary syndrome. *Diabetic Medicine*, *30*(12), 1495–1499. <https://doi.org/10.1111/dme.12262>.
- Sampaio, A. F., Silva, M., Dornas, W. C., Costa, D. C., Silva, M. E., Dos Santos, R. C., et al. (2014). Iron toxicity mediated by oxidative stress enhances tissue damage in an animal model of diabetes. *BioMetals*, *27*(2), 349–361. <https://doi.org/10.1007/s10534-014-9717-8>.
- Schrag, M., Mueller, C., Zabel, M., Crofton, A., Kirsch, W. M., Ghribi, O., et al. (2013). Oxidative stress in blood in Alzheimer's disease and mild cognitive impairment: a meta-analysis. *Neurobiology of Disease*, *59*, 100–110. <https://doi.org/10.1016/j.nbd.2013.07.005>.
- Schweser, F., Sommer, K., Deistung, A., & Reichenbach, J. R. (2012). Quantitative susceptibility mapping for investigating subtle susceptibility variations in the human brain. *Neuroimage*, *62*(3), 2083–2100. <https://doi.org/10.1016/j.neuroimage.2012.05.067>.
- Smith, M. A., Harris, P. L., Sayre, L. M., & Perry, G. (1997). Iron accumulation in Alzheimer disease is a source of redox-generated free radicals. *Proceedings of the National Academy of Sciences of the United States of America*, *94*(18), 9866–9868.
- Smith, M. A., Zhu, X., Tabaton, M., Liu, G., McKeel, D. W. Jr., Cohen, M. L., et al. (2010). Increased iron and free radical generation in preclinical Alzheimer disease and mild cognitive impairment. *Journal of Alzheimer's Disease*, *19*(1), 363–372. <https://doi.org/10.3233/JAD-2010-1239>.
- van der Graaf, M., Janssen, S. W., van Asten, J. J., Hermus, A. R., Sweep, C. G., Pikkemaat, J. A., et al. (2004). Metabolic profile of the hippocampus of Zucker diabetic fatty rats assessed by in vivo 1H magnetic resonance spectroscopy. *NMR in Biomedicine*, *17*(6), 405–410. <https://doi.org/10.1002/nbm.896>.
- Wahlund, L. O., Barkhof, F., Fazekas, F., Bronge, L., Augustin, M., Sjøgren, M., et al. (2001). A new rating scale for age-related white matter changes applicable to MRI and CT. *Stroke*, *32*(6), 1318–1322.
- Wang, H., Li, H., Jiang, X., Shi, W., Shen, Z., & Li, M. (2014). Hepcidin is directly regulated by insulin and plays an important role in iron overload in streptozotocin-induced diabetic rats. *Diabetes*, *63*(5), 1506–1518. <https://doi.org/10.2337/db13-1195>.
- Whiting, D. R., Guariguata, L., Weil, C., & Shaw, J. (2011). IDF diabetes atlas: global estimates of the prevalence of diabetes for 2011 and 2030. *Diabetes Research and Clinical Practice*, *94*(3), 311–321. <https://doi.org/10.1016/j.diabres.2011.10.029>.
- Xia, S., Zheng, G., Shen, W., Liu, S., Zhang, L. J., Haacke, E. M., et al. (2015). Quantitative measurements of brain iron deposition in cirrhotic patients using susceptibility mapping. *Acta Radiologica*, *56*(3), 339–346. <https://doi.org/10.1177/0284185114525374>.
- Yan, S., Sun, J., Chen, Y., Selim, M., & Lou, M. (2013). Brain iron deposition in white matter hyperintensities: a 3-T MRI study. *Age (Dordr)*, *35*(5), 1927–1936. <https://doi.org/10.1007/s11357-012-9487-6>.
- Zein, S., Rachidi, S., & Hininger-Favier, I. (2014). Is oxidative stress induced by iron status associated with gestational diabetes mellitus? *Journal of Trace Elements in Medicine and Biology*, *28*(1), 65–69. <https://doi.org/10.1016/j.jtemb.2013.09.009>.
- Zhang, Y. W., Zhang, J. Q., Liu, C., Wei, P., Zhang, X., Yuan, Q. Y., et al. (2015). Memory dysfunction in type 2 diabetes mellitus correlates with reduced hippocampal CA1 and subiculum volumes. *Chinese Medical Journal (Engl)*, *128*(4), 465–471. <https://doi.org/10.4103/0366-6999.151082>.
- Zheng, T., Qin, L., Chen, B., Hu, X., Zhang, X., Liu, Y., et al. (2016). Association of plasma DPP4 activity with mild cognitive impairment in elderly patients with type 2 diabetes: results from the GDMD study in China. *Diabetes Care*, *39*(9), 1594–1601. <https://doi.org/10.2337/dc16-0316>.
- Zhou, Y., Fang, R., Liu, L. H., Chen, S. D., & Tang, H. D. (2015). Clinical characteristics for the relationship between type-2 diabetes mellitus and cognitive impairment: a cross-sectional study. *Aging and Disease*, *6*(4), 236–244. <https://doi.org/10.14336/ad.2014.1004>.